Gold Complexes

DOI: 10.1002/ange.201209140

Generation and Structural Characterization of a Gold(III) Alkene Complex**

*Eirin Langseth, Margaret L. Scheuermann, David Balcells, Werner Kaminsky, Karen I. Goldberg, Odile Eisenstein, Richard H. Heyn, and Mats Tilset**

Gold complexes are effective catalysts for a range of organic transformations including the coupling of alkenes and alkynes to other organic fragments.[1–10] A key step in these catalytic reactions is assumed to be the coordination of a C−C multiple bond to the gold center.[1,2,6] Although various catalytic cycles involving Au^{III} π complexes have been proposed,[2,6,11,12] no Au^{III} alkene,[13] alkyne, allene, or arene complexes have been conclusively detected and characterized.[1,6,14,15] In 1964, Chalk proposed the generation of $[C_8H_{12}{\cdot}AuCl_3]$,[16] based solely on an IR spectrum and elemental analysis of mixtures containing two species.[14,15] Since then several groups have attempted to prepare olefin complexes of Au^{III} chlorides and bromides, but clear identification of an Au^{III} alkene complex has been elusive.[14,15,17–21] Gas phase calculations of $AuCl_3$ and ethylene suggest that the alkene binding is exothermic.[22,23] In contrast, Au^{I} alkene complexes have been known for some time with several examples reported[16,24–32] and in part reviewed.[1–3,33–35]

Recent interest in the characterization of potential Au^{III} intermediates has resulted in the isolation of both an Au^{III} hydride[36] and an Au^{III} vinyl[37] complex. Herein, we describe the preparation of the first crystallographically characterized Au^{III} alkene complex and discuss the factors that contribute to the stability of this unusual molecule, in which the Au center is directly bonded solely to carbon atoms.

The cyclometalated tolylpyridine (tpyH) complex $[(tpy)AuMe_2]$ (**1**, Scheme 1) was prepared as recently described.[38] Addition of triflic acid (HOTf, ca. 2.2 equiv) to a CD_2Cl_2 solution of **1** at −78 °C followed by warming to −40 °C yielded the Au^{III} dimethyl species $[(tpyH)AuMe_2(OTf)]$ (**2**).[39] Selective protonolysis of the Au−C(sp²) bond, as has been observed in other Au^{III} complexes,[40] is confirmed by the two inequivalent AuMe groups, the absence of methane, and the symmetry of the tolyl group. NOE interactions between the protons of one AuMe group and aromatic protons of tpyH suggest that tpyH is coordinated to Au as a monodentate ligand in **2** through the N atom. Triflate presumably occupies the fourth site of the square plane around the Au^{III} center.

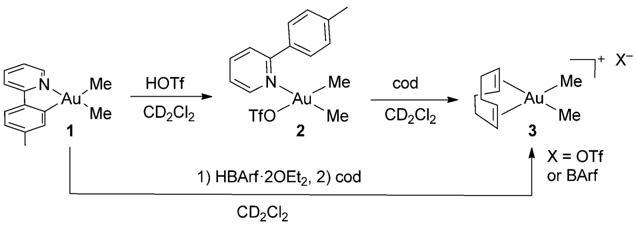

Scheme 1. Protonation of $[(tpy)AuMe_2]$ **1** at low temperature followed by addition of cod to generate $[(cod)AuMe_2^{+}][X^{-}]$ (**3**-X; X = OTf or BArf). BArf = tetrakis[3,5-bis(trifluoromethyl)phenyl]borate.

Addition of 1,5-cyclooctadiene (cod, 1 equiv) to the solution of **2** at −78 °C followed by slow warming to 0 °C resulted in the gradual consumption of cod with concomitant formation of the Au^{III} alkene complex $[(cod)AuMe_2^{+}][OTf^{-}]$ (**3**-OTf; Scheme 1) in 85 % yield from **1** (NMR, internal standard). The byproduct is tolylpyridinium triflate, $tpyH_2OTf$, formed by reaction of HOTf with tpyH liberated from the Au center upon coordination of cod.

The ^1H NMR spectrum of **3**-OTf at 0 °C consists of a single AuMe resonance at $\delta = 1.71$, a pair of multiplets for the CH_2 groups in the backbone of the bound cod at $\delta = 2.75$ and 2.99, and a broad singlet for the vinylic protons of the bound cod at $\delta = 6.39$, which is 0.8 ppm higher than the signal of free cod in CD_2Cl_2 at $\delta = 5.56$. Although vinylic protons typically shift to lower δ values on binding to a metal center,[41] as seen in the Au^{I} complex $[(HB\{3,5\text{-}(CF_3)_2pz\}_3)Au(C_2H_4)]$,[31] there are also examples of shifts to higher δ values with especially electron-deficient metals, such as Ag^{I} in $[(HB\{3,5\text{-}(CF_3)_2tz\}_3)Ag$-

---

[*] Dr. D. Balcells, Prof. M. Tilset
Centre for Theoretical and Computational Chemistry (CTCC)
Department of Chemistry, University of Oslo
P.O. Box 1033 Blindern, 0315 Oslo (Norway)
E-mail: mats.tilset@kjemi.uio.no

E. Langseth[+]
Department of Chemistry, University of Oslo, Oslo (Norway)

M. L. Scheuermann,[+] Prof. W. Kaminsky, Prof. K. I. Goldberg
Department of Chemistry, University of Washington, Seattle (USA)

Dr. R. H. Heyn
SINTEF Materials and Chemistry, Oslo (Norway)

Prof. O. Eisenstein
Institut Charles Gerhardt, UMR 5253 CNRS Université Montpellier 2
Montpellier (France)
and
Centre for Theoretical and Computational Chemistry (CTCC)
Department of Chemistry, University of Oslo, Oslo (Norway)

[+] These authors contributed equally to this work.

[**] This work was supported by the National Science Foundation under grants no. DGE-0718124 and CHE-1012045, the Research Council of Norway, grants no. 185513/I30 and 212030/F11 (travel grant to M.S.), and the University of Oslo with a Kristine Bonnevie travel grant to E.L.

Supporting information for this article is available on the WWW under http://dx.doi.org/10.1002/anie.201209140.

(C_2H_4)] (pz = pyrazolyl, tz = triazolyl).[42] The signal of the ethylene protons of this Ag complex appears 0.3 ppm higher than that of free ethylene. Notably, the ^{13}C resonance for the bound ethylene shifts to lower values by 13.6 ppm. In **3**-OTf the ^{13}C signal of the cod sp^2 carbon atoms is also shifted to a higher δ value, 134 ppm when compared to free cod at $\delta = 129$. Further support for the binding of cod to gold is a through-space NOE interaction (700 MHz, 233 K) between the vinylic protons of the bound cod and the AuMe groups.

The stability of **3**-OTf at ambient temperature in solution is somewhat limited. After 12 h at 25 °C, the concentration of **3**-OTf (initially ca. 14 mM) decreased by approximately 50 % even with a cod concentration of 40 mM in CD_2Cl_2. Attempts to obtain crystals from reaction mixtures containing **3**-OTf and excess HOTf invariably led to isolation of tpyH_2OTf.

In an effort to isolate crystals of the Au^{III} alkene complex, the reaction was repeated using 0.9 equivalent of HOTf to suppress the formation of tpyH_2OTf in the reaction mixture. However, the subsequent addition of as much as 50 equivalents of cod resulted in only approximately 30 % yield of the desired **3**-OTf (NMR, internal standard). In addition, the reaction mixture contained **2** (ca. 20 %) and a new species (ca. 20 %) that was subsequently identified as [(tpyH)$_2$AuMe$_2^+$][OTf$^-$] (**4**-OTf) by comparison to an independently prepared and crystallographically characterized sample.[39,43] Upon addition of tpyH (ca. 6 equiv) to the equilibrium mixture above, the composition of the reaction mixture changed to < 5 % yield of **3**-OTf, approximately 20 % of **2**, and approximately 60 % of **4**-OTf. These observations suggest that **2**, **3**-OTf, **4**-OTf, free cod, and free tpyH are in equilibrium, that is, cod and tpyH compete for coordination sites at the Au^{III} moiety. Importantly, the ^1H NMR resonances of **3**-OTf remain unchanged regardless of whether the other species present in the reaction mixture are tpyH_2OTf (resulting from excess acid) or **2** and **4**-OTf (less than 1 equiv of acid). From this observation we infer that **3**-OTf does not have an associated tpyH ligand in solution. All attempts to obtain crystals from reaction mixtures without excess HOTf resulted only in crystals of **4**-OTf.[39]

When approximately one equivalent of [{3,5-(CF_3)$_2$-C_6H_3}$_4$B$^-$][(Et_2O)$_2$H$^+$] (HBArf·2 OEt$_2$)[44] was used for the protonolysis of **1** in CD_2Cl_2, followed by addition of 15 equivalents of cod, [(cod)AuMe$_2^+$][BArf$^-$] (**3**-BArf) was generated in approximately 70 % yield (NMR, internal standard). The ^1H NMR chemical shifts for the AuMe groups and the vinylic and CH_2 protons of bound cod in **3**-BArf appear within 0.2 ppm of the corresponding resonances in a spectrum of **3**-OTf. The solution containing **3**-BArf was layered with pentane and left in a freezer at −35 °C, resulting in small crystalline demispheres suitable for X-ray diffraction. The structure of the cation of **3**-BArf is shown in Figure 1.[43]

Compound **3**-BArf crystallized in the monoclinic space group $P2_1/c$ with the Au cation sitting in a pocket formed by the aryl groups of several BArf$^-$ anions.[43] The Au−C_{cod} bonds are rather long for a metal alkene complex, 2.389 Å (avg.). The cation is nearly C_2 symmetric (not crystallographically imposed). Interestingly, each cod C=C bond is asymmetrically bonded to Au such that one Au−C bond is significantly longer than the other (2.362(4) vs. 2.406(4) and 2.371(4) vs. 2.415(4) Å, respectively). The C=C bond lengths in **3**-BArf are 1.348(5) and 1.364(5) Å. Several cationic Au^I alkene complexes have been recently structurally characterized.[24–30,32] Their Au−C_{alkene} bond lengths are in the range of 2.098(5)[24]–2.37(1)[30] Å, and the C=C distances are in the range of 1.319[26]–1.409(4)[25] Å. It is noteworthy that the two long Au−C_{cod} distances in the cationic Au^{III} complex **3**-BArf are longer than the longest Au−C_{alkene} distances in the structurally characterized, cationic Au^I complexes.[24–30,32] Furthermore, the C=C distances in **3**-BArf are essentially in the middle of the range seen for these Au^I complexes, thus indicating some back-bonding from Au^{III} to the C=C bonds, despite the strong *trans* influence of the two methyl groups.

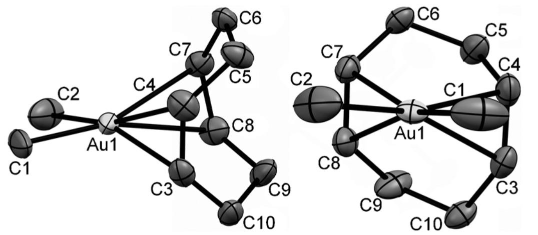

Figure 1. Two ORTEP views of the Au^{III} cation in the 100 K solid-state structure of **3**-BArf with 50 % probability ellipsoids. Hydrogen atoms are omitted for clarity. Selected bond lengths [Å] and angles [°]: Au(1)–C(1) 2.049(4), Au(1)–C(2) 2.055(4), Au(1)–C(3) 2.371(4), Au(1)–C(4) 2.415(4), Au(1)–C(7) 2.362(4), Au(1)–C(8) 2.406(4), C(3)–C(4) 1.348(5), C(7)–C(8) 1.364(5); C(3)-Au(1)-C(4) 32.71(13), C(7)-Au(1)-C(8) 33.23(12), C(7)-Au(1)-C(4) 77.86(13), C(3)-Au(1)-C(8) 77.87(13), C(1)-Au(1)-C(2) 85.0(2).

The Au−C_{cod} bonds in **3**-BArf are also considerably longer than the Pt−C_{cod} bonds in the isoelectronic Pt^{II} complex [(cod)PtMe$_2$], and the C=C distances are significantly shorter in the Au complex than in the Pt analogue (Table 1), thereby hinting at reduced back-bonding from d(M) to π*(cod) orbitals when Au^{III} is compared to Pt^{II}. The Au−C_{Me} bond lengths in **3**-BArf are 2.049(4) and 2.055(4) Å, quite typical for cationic $Au^{III}Me_2$ fragments with relatively weak donor ligands *trans* to the methyl groups.[45,46]

The structures of [(cod)AuMe$_2^+$] and [(cod)PtMe$_2$], optimized at the DFT level with the hybrid PBE0 functional and quasi relativistic effective core potential (ECP) for Au (see computational details[47]), indispensable for representing the structures and reactivity of Au complexes,[57,58] are in excellent agreement with the solid-state structures (Table 1 and the Supporting Information). In particular, the calculations reproduce very well the nonequivalence of the two M−C_{cod} bond lengths to the same C=C, and the larger difference between these distances for Au versus Pt. For [(cod)AuMe$_2^+$], the distances differ by 0.052 Å, but for [(cod)PtMe$_2$] they differ by only 0.024 Å. In relation to this, the olefinic carbon atoms C3, C4, C7, and C8 are not coplanar; the calculated dihedral angles C3-C4-C7-C8 are 13.7° and 11.6° for Au^{III} and Pt^{II}, respectively. These calculated values are in excellent agreement with the solid-state values of 13.4° and 12.7°, which show that these structural features are not due to crystal packing or to the counteranion in the case of Au^{III}, since the geometries were

Table 1: Selected geometrical parameters for [(cod)AuMe$_2^+$], [(cod)PtMe$_2$], and free cod, and distortion energies of the cod ligand.[a] See Figure 1 for atom labels.

	[(cod)AuMe$_2^+$]		[(cod)PtMe$_2$]		cod	
	Exp.[b]	Theo.[c]	Exp.[d]	Theo.[c]	Exp.[e]	Theo.[c]
Distances [Å]						
M–C1[f]	2.049(4)	2.055	2.040(11)	2.057	–	–
M–C2[f]	2.055(4)	2.055	2.072(11)	2.057	–	–
M–C3 (d$_1$)[f]	2.362(4)	2.390	2.204(11)	2.211	–	–
M–C4 (d$_2$)[f]	2.406(4)	2.442	2.255(12)	2.235	–	–
Δ(d$_2$–d$_1$)	0.044	0.052	0.051	0.024	–	–
M–C7 (d$_3$)[f]	2.371(4)	2.390	2.224(11)	2.211	–	–
M–C8 (d$_4$)[f]	2.415(4)	2.442	2.230(11)	2.235	–	–
Δ(d$_4$–d$_3$)	0.044	0.052	0.006	0.024	–	–
Δ(avg.)[g]	0.044	0.052	0.029	0.024	–	–
C3–C4	1.364(5)	1.366	1.348(17)	1.385	1.340(3)	1.335
C7–C8	1.348(5)	1.366	1.361(17)	1.385	1.340(3)	1.335
Angles [°]						
C3-C4-C7-C8	13.4	13.7	12.7	11.6	20.2	23.6
C4-C5-C6-C7	46.5	44.4	34.5	36.7	63.8	61.2
C8-C9-C10-C3	42.6	44.4	33.1	36.7	63.8	61.2
E [kcal mol^{-1}]						
Distortion E[h]	–	4.7	–	12.7	–	0.0

[a] Distances [Å], angles [°], energies (kcal mol^{-1}). [b] X-ray structure reported in this work. [c] DFT (PBE0) calculations;[47] [d] Data from X-ray structure.[54] An earlier determined structure, for which the cif file is not available, gives a Δ(avg.) of 0.024 Å;[55] [e] Data from gas-phase electron diffraction structure;[56] [f] M = Au, Pt; [g] Mean value of Δ(d$_2$–d$_1$) and Δ(d$_4$–d$_3$); [h] Energy difference, *E*(bound)–*E*(free), between optimized free cod and cod in the confirmations calculated in [(cod)AuMe$_2^+$] and [(cod)PtMe$_2$], respectively.

fully optimized in the gas phase and in the absence of a counteranion. To determine the origin of these features, free cod was optimized at the same level of theory. In free cod, the C3-C4-C7-C8 dihedral angle is 23.6°, showing that the two C=C bonds are distinctively nonparallel. It thus appears that the two C=C bonds become increasingly parallel upon coordination and more so for Pt^{II} than Au^{III}. This trend is attributed to the preference for a staggered conformation of the -CH$_2$CH$_2$- backbone of cod. In free cod where no constraints are present, the two -CH$_2$CH$_2$- units are fully staggered as indicated by the dihedral angles C4-C5-C6-C7 and C8-C9-C10-C3 of 61.2°, associated with the dihedral angle C3-C4-C7-C8 of 23.6°. Coordination of the metal to the two C=C bonds, which forces the two double bonds to be more parallel, also forces the -CH$_2$CH$_2$- linkers to assume a more eclipsed conformation. The effect is smaller for Au^{III} than Pt^{II} as shown by the C4-C5-C6-C7 and C8-C9-C10-C3 dihedral angles of 45° and 35° (avg.), respectively. The -CH$_2$CH$_2$- backbone never reaches a fully eclipsed conformation and the two C=C bonds never become coplanar, which leads to nonequivalent M–C bond lengths.

Distorting the cod ligand from its preferred conformation to its conformations in the metal complexes has an energy cost of 4.7 kcal mol^{-1} and 12.7 kcal mol^{-1} for Au^{III} and Pt^{II}, respectively. The electronic effect that compensates for this distortion energy is the back donation from the metal to the two π* orbitals as shown by an NBO (natural bond orbital) analysis. The four orbitals containing the 8 d electrons were identified amongst the NLMOs (natural localized molecular orbitals). The d$_{z^2}$ and d$_{x^2-y^2}$ orbitals appear as lone pairs located on the metal center, with no significant contribution from the ligands (see the Supporting Information). In contrast, the d$_{xz}$ and d$_{yz}$ orbitals are involved in the d→π* back donation from the metal center to the C=C bond of cod. This interaction is weaker in [(cod)AuMe$_2^+$], where the contribution from the π*(C=C) (see the Supporting Information) is 2.2% with the d$_{xz}$ and 2.8% with the d$_{yz}$. The corresponding numbers for [(cod)PtMe$_2$] are 9.5% with the d$_{xz}$ and 12% with the d$_{yz}$. The difference between Au and Pt is apparent in the graphical representation of these NLMOs (Figure 2) and is consistent with the greater distortion (more eclipsed) of the -CH$_2$CH$_2$- backbones of cod in the Pt complex and the increasing elongation of the C=C bonds (1.335 Å in free cod, 1.366 Å in [(cod)AuMe$_2^+$], and 1.385 Å in [(cod)PtMe$_2$]). These results show that, compared to Pt, the metal d→π*(C=C) back donation is weaker, but still significant, in [(cod)AuMe$_2^+$], thus stabilizing this unprecedented Au^{III} bis(alkene) complex.

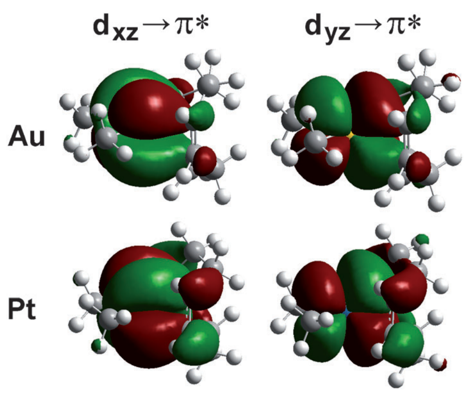

Figure 2. NLMOs (with orbital phases in green/red) associated with the metal d→π*(cod) back donation.

In summary, we have successfully characterized the first Au^{III} alkene complex, including the crystal structure of [(cod)AuMe$_2^+$][BArf$^-$]. This unambiguous demonstration of the existence of Au^{III} alkene complexes validates their inclusion in mechanistic proposals and will allow for further work to better understand mechanisms that potentially involve Au^{III} alkene complexes. Reactivity studies of **3**-OTf along with improved synthesis of this and other Au^{III} complexes with π-bound ligands are currently under investigation.

Received: November 14, 2012

Keywords: density functional calculations · gold · gold(III) alkene · homogeneous catalysis · reactive intermediates

[1] A. S. K. Hashmi, *Angew. Chem.* **2010**, *122*, 5360–5369; *Angew. Chem. Int. Ed.* **2010**, *49*, 5232–5241.
[2] A. S. K. Hashmi, *Chem. Rev.* **2007**, *107*, 3180–3211.
[3] A. S. K. Hashmi, G. J. Hutchings, *Angew. Chem.* **2006**, *118*, 8064–8105; *Angew. Chem. Int. Ed.* **2006**, *45*, 7896–7936.
[4] M. Rudolph, A. S. K. Hashmi, *Chem. Soc. Rev.* **2012**, *41*, 2448–2462.
[5] A. Arcadi, *Chem. Rev.* **2008**, *108*, 3266–3325.
[6] H. Schmidbaur, A. Schier, *Arabian J. Sci. Eng.* **2012**, *37*, 1187–1225.
[7] V. K.-Y. Lo, K. K.-Y. Kung, M.-K. Wong, C.-M. Che, *J. Organomet. Chem.* **2009**, *694*, 583–591.
[8] Z. Li, C. Brouwer, C. He, *Chem. Rev.* **2008**, *108*, 3239–3265.
[9] A. Fürstner, P. W. Davies, *Angew. Chem.* **2007**, *119*, 3478–3519; *Angew. Chem. Int. Ed.* **2007**, *46*, 3410–3449.
[10] N. D. Shapiro, F. D. Toste, *Synlett* **2010**, 675–691.
[11] R.-V. Nguyen, X. Yao, C.-J. Li, *Org. Lett.* **2006**, *8*, 2397–2399.
[12] Y.-P. Xiao, X.-Y. Liu, C.-M. Che, *J. Organomet. Chem.* **2009**, *694*, 494–501.
[13] After submission of this manuscript, a report on Au^{III} alkene complexes characterized by NMR appeared: N. Savjani, D.-A. Roşca, M. Schormann, M. Bochmann, *Angew. Chem.* **2012**, DOI: 10.1002/ange.201208356; *Angew. Chem. Int. Ed.* **2012**, DOI: 10.1002/anie.201208356.
[14] H. Schmidbaur, A. Schier, *Organometallics* **2010**, *29*, 2–23.
[15] R. O. C. Norman, W. J. E. Parr, C. B. Thomas, *J. Chem. Soc. Perkin Trans. 1* **1976**, 811–817.
[16] A. J. Chalk, *J. Am. Chem. Soc.* **1964**, *86*, 4733–4734.
[17] R. O. C. Norman, W. J. E. Parr, C. B. Thomas, *J. Chem. Soc. Perkin Trans. 1* **1976**, 1983–1987.
[18] F. H. Brain, C. S. Gibson, J. A. J. Jarvis, R. F. Phillips, H. M. Powell, A. Tyabji, *J. Chem. Soc.* **1952**, 3686–3694.
[19] P. K. Monaghan, R. J. Puddephatt, *Inorg. Chim. Acta* **1975**, *15*, 231–234.
[20] B. Armer, H. Schmidbaur, *Angew. Chem.* **1970**, *82*, 120–133; *Angew. Chem. Int. Ed. Engl.* **1970**, *9*, 101–113.
[21] H. Schmidbaur, *Angew. Chem.* **1976**, *88*, 830–843; *Angew. Chem. Int. Ed. Engl.* **1976**, *15*, 728–740.
[22] M. García-Mota, N. Cabello, F. Maseras, A. M. Echavarren, J. Pérez-Ramírez, N. Lopez, *ChemPhysChem* **2008**, *9*, 1624–1629.
[23] R. Kang, H. Chen, S. Shaik, J. Yao, *J. Chem. Theory Comput.* **2011**, *7*, 4002–4011.
[24] M. A. Cinellu, G. Minghetti, S. Stoccoro, A. Zucca, M. Manassero, *Chem. Commun.* **2004**, 1618–1619.
[25] M. A. Cinellu, G. Minghetti, F. Cocco, S. Stoccoro, A. Zucca, M. Manassero, M. Arca, *Dalton Trans.* **2006**, 5703–5716.
[26] T. J. Brown, M. G. Dickens, R. A. Widenhoefer, *Chem. Commun.* **2009**, 6451–6453.
[27] T. J. Brown, M. G. Dickens, R. A. Widenhoefer, *J. Am. Chem. Soc.* **2009**, *131*, 6350–6351.
[28] T. N. Hooper, M. Green, J. E. McGrady, J. R. Patel, C. A. Russell, *Chem. Commun.* **2009**, 3877–3879.
[29] R. E. M. Brooner, R. A. Widenhoefer, *Organometallics* **2011**, *30*, 3182–3193.
[30] R. E. M. Brooner, R. A. Widenhoefer, *Organometallics* **2012**, *31*, 768–771.
[31] H. V. R. Dias, J. Wu, *Angew. Chem.* **2007**, *119*, 7960–7962; *Angew. Chem. Int. Ed.* **2007**, *46*, 7814–7816.
[32] H. V. R. Dias, M. Fianchini, T. R. Cundari, C. F. Campana, *Angew. Chem.* **2008**, *120*, 566–569; *Angew. Chem. Int. Ed.* **2008**, *47*, 556–559.
[33] H. V. R. Dias, C. J. Lovely, *Chem. Rev.* **2008**, *108*, 3223–3238.
[34] H. V. R. Dias, J. Wu, *Eur. J. Inorg. Chem.* **2008**, 509–522.
[35] M. A. Cinellu in *Modern Gold Catalyzed Synthesis* (Eds.: A. S. K. Hashmi, F. D. Toste), Wiley-VCH, Weinheim, **2012**, pp. 175–199.
[36] D.-A. Roşca, D. A. Smith, D. L. Hughes, M. Bochmann, *Angew. Chem.* **2012**, *124*, 10795–10798; *Angew. Chem. Int. Ed.* **2012**, *51*, 10643–10646.
[37] O. A. Egorova, H. Seo, Y. Kim, D. Moon, Y. M. Rhee, K. H. Ahn, *Angew. Chem.* **2011**, *123*, 11648–11652; *Angew. Chem. Int. Ed.* **2011**, *50*, 11446–11450.
[38] E. Langseth, C. H. Görbitz, R. H. Heyn, M. Tilset, *Organometallics* **2012**, *31*, 6567–6571.
[39] See the Supporting Information for full experimental and spectroscopic details.
[40] J. K. Jawad, R. J. Puddephatt, M. A. Stalteri, *Inorg. Chem.* **1982**, *21*, 332–337.
[41] R. H. Crabtree, *The Organometallic Chemistry of the Transition Metals*, 5th ed., Wiley, Hoboken, **2005**.
[42] X. Kou, H. V. R. Dias, *Dalton Trans.* **2009**, 7529–7536.
[43] CCDC 910693 (**3**-BArf) and 910694 (**4**-OTf) contains the supplementary crystallographic data for this paper. These data can be obtained free of charge from The Cambridge Crystallographic Data Centre via www.ccdc.cam.ac.uk/data_request/cif.
[44] M. Brookhart, B. Grant, A. F. Volpe, Jr., *Organometallics* **1992**, *11*, 3920–3922. Differing from the description in this reference, the material used by us was found to have an additional 4 equiv of Et_2O associated.
[45] A. Venugopal, M. K. Ghosh, H. Jürgens, K. W. Törnroos, O. Swang, M. Tilset, R. H. Heyn, *Organometallics* **2010**, *29*, 2248–2253.
[46] A. J. Canty, N. J. Minchin, P. C. Healy, A. H. White, *J. Chem. Soc. Dalton Trans.* **1982**, 1795–1802.
[47] The calculations were carried out at the DFT level with Gaussian 09.[48] C and H were described with the all-electron triple-ζ 6-311 + G** basis set,[49,50] whereas Au was described with the new Stuttgart–Köln basis set including a small-core quasi-relativistic pseudopotential.[51] Geometries were fully optimized without any constraint. Vibrational frequencies were computed analytically to verify that the stationary points found were minima. Several functionals were used (see the Supporting Information) and PBE0[52] gave the lowest root-mean-square deviation from the experimental X-ray Au–C bond lengths. PBE0 was also selected in a recent study of Au^{I} and Au^{III} alkene complexes, based on reference coupled cluster calculations.[23] The geometry optimization of [(cod)$PtMe_2$] and the NBO (5.9 version) analysis[53] were thus carried out with PBE0.
[48] Gaussian 09 (Revision B.01): M. J. Frisch et al., see the Supporting Information.
[49] A. D. McLean, G. S. Chandler, *J. Chem. Phys.* **1980**, *72*, 5639–5648.
[50] R. Krishnan, J. S. Binkley, R. Seeger, J. A. Pople, *J. Chem. Phys.* **1980**, *72*, 650–654.
[51] D. Figgen, G. Rauhut, M. Dolg, H. Stoll, *Chem. Phys.* **2005**, *311*, 227–244.
[52] C. Adamo, V. Barone, *J. Chem. Phys.* **1999**, *110*, 6158–6170.
[53] A. E. Reed, L. A. Curtiss, F. Weinhold, *Chem. Rev.* **1988**, *88*, 899–926.
[54] R. P. Hughes, J. S. Overby, K.-C. Lam, C. D. Incarvito, A. L. Rheingold, *Polyhedron* **2002**, *21*, 2357–2360.
[55] A. Klein, K.-W. Klinkhammer, T. Scheiring, *J. Organomet. Chem.* **1999**, *592*, 128–135.
[56] K. Hagen, L. Hedberg, K. Hedberg, *J. Phys. Chem.* **1982**, *86*, 117–121.
[57] M. Pernpointner, A. S. K. Hashmi, *J. Chem. Theory Comput.* **2009**, *5*, 2717–2725.
[58] M. Lein, M. Rudolph, A. S. K. Hashmi, P. Schwerdtfeger, *Organometallics* **2010**, *29*, 2206–2210.